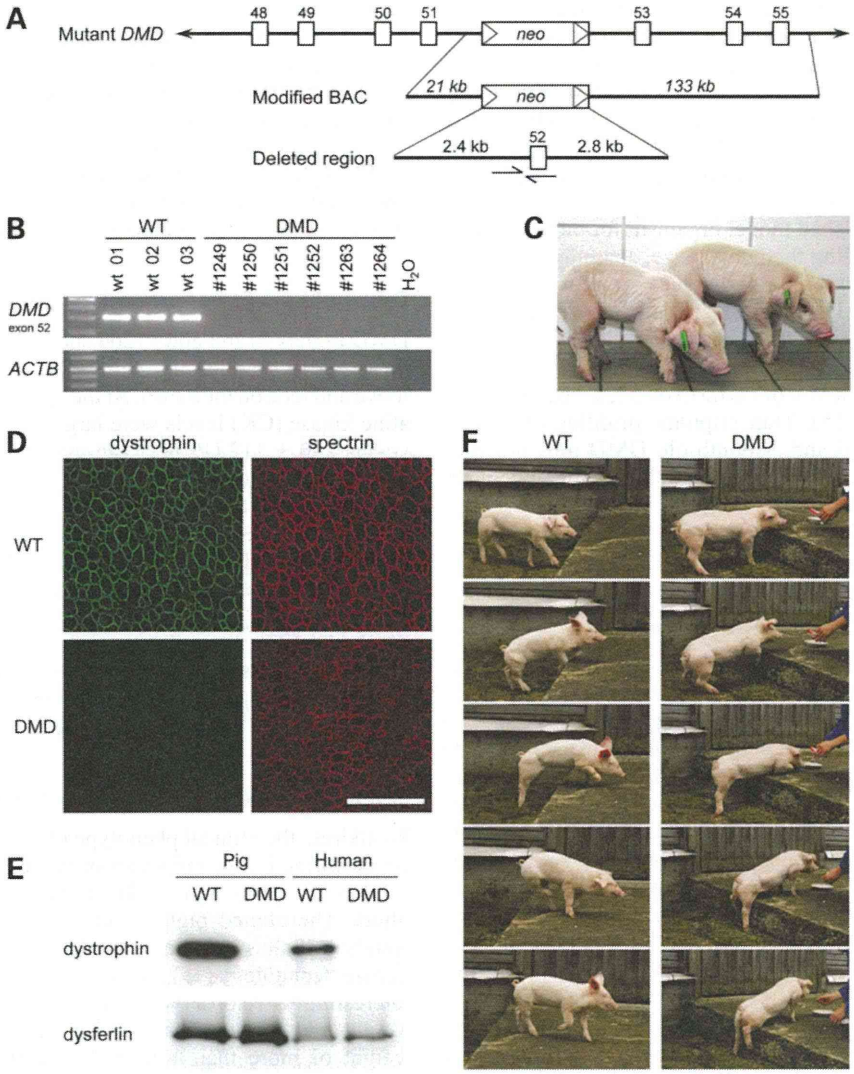

Figure 1. Targeted deletion of exon 52 of the porcine *DMD* gene and consequences for dystrophin expression and muscle function. (**A**) Schematic picture of replacement of exon 52 by a *neo*® cassette to generate the targeting BAC. The primers used to detect the loss of exon 52 are indicated as arrows. (**B**) Genomic PCR analysis demonstrating the loss of *DMD* exon 52 in cloned piglets; WT, wild-type; *ACTB*, β-actin gene. (**C**) Ten-day-old *DMD* mutant pigs. (**D**) Immunofluorescence analysis demonstrating lack of dystrophin expression in biceps femoris muscle of a DMD pig. Anti-spectrin antibodies were used for membrane staining; original magnification ×400; bar = 50 μm. (**E**) Western blot confirming the absence of dystrophin in a DMD pig and a human DMD patient. Anti-dysferlin antibodies were used to control for equal loading within species. (**F**) Inability of a 9-week-old DMD pig to climb a 25 cm platform, demonstrating striking muscle weakness.

myopathy with excessive fibre size variation, numerous large rounded hypertrophic fibres, branching fibres and fibres with central nuclei, as well as scattered clusters of segmentally necrotic fibres, next to hypercontracted fibres and groups of small regenerating muscle fibres. These lesions were accompanied by interstitial fibrosis and mononuclear inflammatory cell infiltration, mimicking the hallmarks of the human disease. The severity and extent of these alterations progressed with age (Fig. 2B) and was most severe in the diaphragm, the laryngeal and intercostal musculature, and triceps brachii muscle. Examination of the heart musculature did not reveal accentuated signs for a cardiac involvement (Fig. 2C).

Morphometric analyses were performed on samples of biceps femoris muscle of 2-day-old and 3-month-old DMD and WT pigs (Fig. 3A). The mean minimal Feret's diameter of muscle fibres was 34% ($P < 0.01$) and 55% ($P < 0.001$) reduced in 2-day-old and 3-month-old DMD pigs when compared with age-matched WT controls (Fig. 3B). Further, the proportion of muscle fibre cross-section profiles with centrally located nuclear section profiles was doubled in 2-day-old DMD pigs and was increased by more than 20-fold in 3-month-old DMD pigs (Fig. 3B). The distribution of muscle fibre diameters from the mean was similar in 2-day-old DMD and WT pigs (Fig. 3C, left panel). In contrast, 3-month-old DMD pigs displayed a broadened, biphasic distribution, with peaks in small and large diameters of fibre size (Fig. 3C, right panel), indicating progressive DMD pathology.

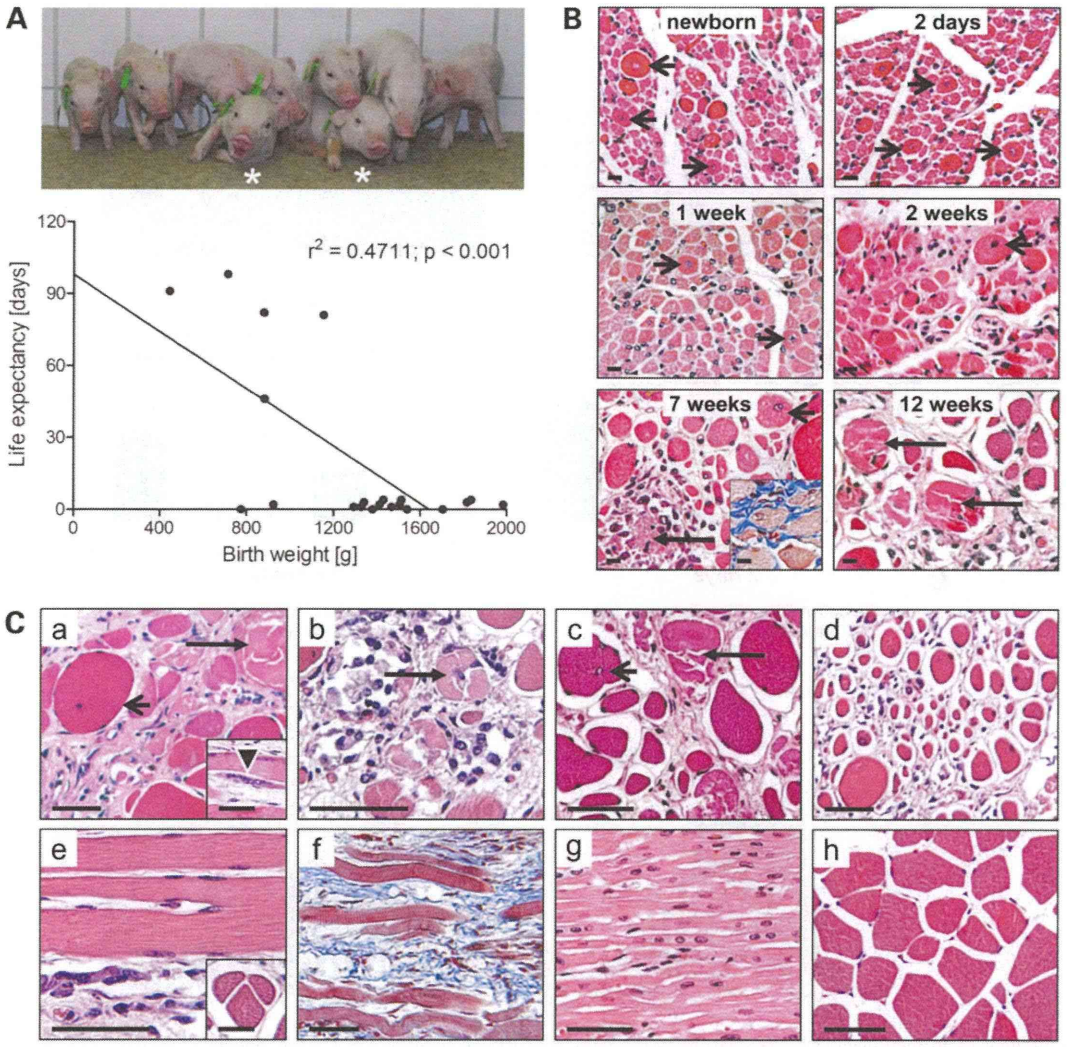

Figure 2. Birth weight, life expectancy and pathological alterations of DMD pigs. (**A**) A significant negative correlation between birth weight and life expectancy was revealed in the 22 DMD pigs of the second series of cloning experiments. Representative pigs are shown in the photograph. Note that pigs with a high birth weight between 1820 and 1980 g (marked by asterisks) were not able to stand or to move (see also Supplementary Material, Video S2). (**B**) Age-related progression of severity of structural alterations in skeletal muscle of DMD pigs of different ages as indicated. Histology of the biceps femoris muscle, paraffin sections, haematoxylin and eosin (H&E)-staining; inset: demonstration of interstitial fibrosis by Masson's trichrome-staining (blue colour). Short arrows indicate large, rounded fibres with internalized central nuclei, long arrows necrosis of muscle fibres. Bars = 10 μm. (**C**) Histopathology of muscles of 3-month-old DMD pigs (a–g) and an age-matched control pig (h). Paraffin sections. H&E-staining (a–e, g, h), Masson's trichrome-staining (f). Bars = 50 μm, bar in inset to e = 10 μm. Cross-sections of the triceps brachii muscle (a, h), the diaphragm (left pillar, b), thyreohyoideus muscle (larynx, c) and longissimus dorsi muscle (d) demonstrating excessive variation of fibre diameters with hypertrophic rounded fibres with centrally located nuclei (short arrows), regeneration of fibres (arrowhead in inset to a) and necrosis of muscle fibres (long arrows) with peri- and endomysial mononuclear (histiocytic) cell infiltration (b). (e) (triceps brachii muscle, longitudinal section; inset: biceps femoris muscle, cross section): Branching/splitting of fibres. (f) (diaphragm, longitudinal section): interstitial fibrosis (blue colour). (g) (heart, left ventricle, longitudinal section): Normal histomorphology.

In summary, the clinical and pathological studies indicate that DMD pigs develop a progressive muscular dystrophy in an accelerated mode when compared with human patients.

Differential expression and localization of utrophin in young versus older DMD pigs

In DMD patients and in the *mdx* mouse model, an up-regulation of dystrophin-related protein (utrophin) has been observed, which can partially compensate the function of dystrophin (reviewed in 20). Thus, we asked if the level of utrophin expression in DMD pigs may contribute to their accelerated phenotype.

Western blot analysis showed a trend of increased utrophin expression in 2-day-old and markedly increased utrophin levels in 3-month-old DMD pigs when compared with age-matched WT pigs (Fig. 4A).

Immunohistochemistry did not detect sarcolemmal utrophin expression in 2-day-old DMD and WT pigs (Fig. 4B). In both groups, blood vessels were strongly stained, probably representing the main source of signal in the western blot analysis. In

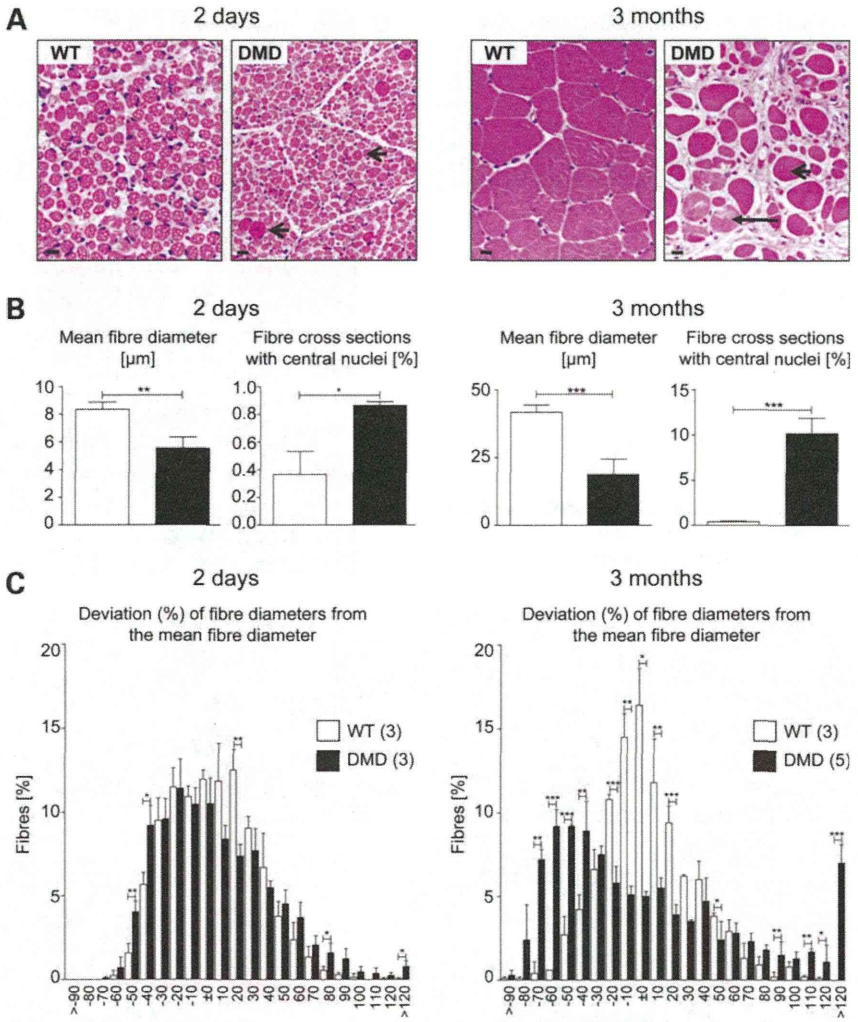

Figure 3. Quantification of structural alterations of skeletal muscle in DMD versus WT pigs at 2 days ($n = 3/3$) and 3 months of age ($n = 5/3$). (**A**) Histology of biceps femoris muscle. Short arrows indicate large, rounded fibres with internalized central nuclei, long arrow necrosis of muscle fibres. Plastic (GMA/MMA) sections, H&E staining; bars = 10 µm. (**B**) Mean minimal Feret's diameter of muscle fibre cross-section profiles (biceps femoris muscle) and proportion of muscle fibre cross-section profiles with central nuclei cross-section profiles. The coefficient of variation in the minimal Feret's diameter was significantly ($P < 0.001$) higher in DMD pigs of both age groups (2 days: 0.38 ± 0.01 versus 0.29 ± 0.02 in WT; 3 months: 0.71 ± 0.05 versus 0.31 ± 0.01 in WT). While the volume density of muscle fibres was not different between 2-day-old DMD and WT piglets, this parameter was significantly ($P < 0.001$) decreased in 3-month-old DMD pigs (0.71 ± 0.04) when compared with age-matched WT pigs (0.96 ± 0.02). (**C**) Distribution of deviations of muscle fibre minimal Feret's diameters from the mean fibre diameter (in classes of 10% deviation) in the biceps femoris muscle. Note the broadened biphasic distribution of muscle fibre diameters in 3-month-old DMD pigs. Data: means ± SD. Significance: $^{*}P < 0.05$; $^{**}P < 0.01$; $^{***}P < 0.001$.

contrast, 3-month-old DMD pigs displayed clear sarcolemmal utrophin staining (Fig. 4B).

Genotype- and age-related transcriptome changes in skeletal muscle

To systematically address the markedly accelerated disease progression in DMD pigs when compared with human DMD patients and *mdx* mouse models, we performed a holistic transcriptome study of biceps femoris muscle from 2-day-old ($n = 4$) and 3-month-old DMD pigs ($n = 3$) and of age-matched WT controls ($n = 3$ per age) using Affymetrix PorGene 1.0 ST arrays. A heat map of the differentially expressed genes (DEGs) among the four groups defined by genotype × age is shown in Figure 5A. The numbers of transcripts with increased and decreased abundance in 2-day-old DMD versus WT pigs were 176 and 67, respectively. The corresponding numbers of DEGs in 3-month-old DMD versus WT pigs were 164 and 35. In addition, a large number of DEGs (77 up- and 148 down-regulated) between 2-day-old and 3-month-old DMD pigs were found (Fig. 5B). These DEGs do not reflect the physiological age-related change of the muscle transcriptome profile, since only 12 (16%) up-regulated and 5 (3%) down-regulated genes were also differentially expressed between 2-day-old and 3-month-old WT pigs (Fig. 5C). Only 11 genes (*LAMA2*, *SMPDL3A*, *PRG4*, *PLSCR4*, *ARID5B*, *ANKRD1*, *ANKRD44*, *TPR*, *CSRP3*, *GABARAPL1*,

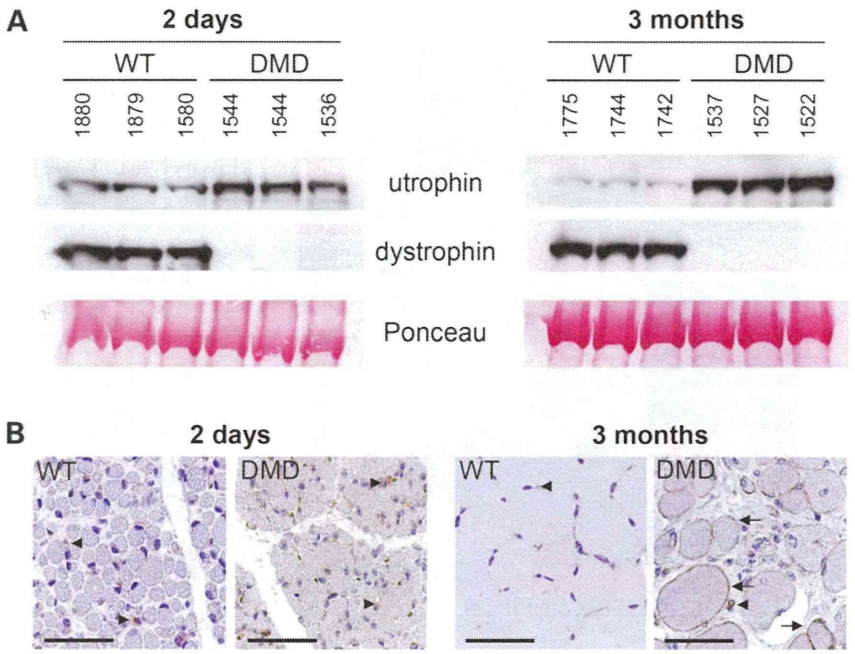

Figure 4. Analysis of utrophin expression in DMD and WT pigs. (**A**) Western blot indicating that utrophin tends to be up-regulated in 2-day-old and is markedly up-regulated in 3-month-old DMD pigs when compared with age-matched WT controls. The Ponceau Red stained membrane is shown to demonstrate equal loading of the lanes. (**B**) Immunohistochemical detection of utrophin in biceps femoris muscle of 2-day-old and 3-month-old DMD pigs and age-matched WT controls. Three-month-old DMD pigs exhibit pronounced sarcolemmal utrophin staining (brown colour, arrows). In 2-day-old DMD and WT pigs, utrophin staining is restricted to blood vessels (arrowheads). Paraffin sections. Bars = 50 μm.

CPM) were commonly overexpressed in both 2-day-old and 3-month-old DMD pigs when compared with age-matched WT pigs, while 5 transcripts (*GADL1*, *MSTN*, *AMPD1*, *EGF*, *DMD*) were reduced in abundance in DMD pigs of both age groups (Fig. 5D), indicating marked differences in the molecular changes associated with the DMD pathology in 2-day-old and 3-month-old animals. Microarray data have been deposited in the GEO database (www.ncbi.nlm.nih.gov/geo/) with the accession number GSE44096.

To get insight into the biological relevance of these transcriptome changes, we performed functional annotation clustering of the DEGs using the Database for Annotation, Visualisation and Integrated Discovery (DAVID) v6.7 (21,22). In addition, we used the tools REVIGO (23) and Cytoscape (24) to visualize enriched gene ontology (GO) terms.

Enriched GO terms for genes overexpressed in 2-day-old DMD versus WT pigs were '(actin) cytoskeleton', 'muscle organ development, actin filament-based movement', 'DNA repair', 'lipid transport' and 'proteolysis' (Fig. 6A; Supplementary Material, Table S1A). GO terms of transcripts with decreased abundance in 2-day-old DMD pigs included 'extracellular matrix', 'extracellular matrix organisation', 'cell adhesion', 'cell cycle/mitosis/cytoskeleton', 'collagen', 'lipid biosynthetic process', 'growth factor', 'vasculature development', 'regulation of cell cycle' and 'regeneration/regulation of growth' (Fig. 6B; Supplementary Material, Table S1B). These transcriptome changes are compatible with the histological findings of muscular dystrophy in the absence of inflammation and fibrosis.

In contrast, highly enriched GO terms of genes overexpressed in biceps femoris muscle of 3-month-old DMD versus WT pigs included 'extracellular region', 'cell adhesion/extracellular matrix', 'lysosome/vacuole', 'proteolysis', 'polysaccharide/heparin binding', 'collagen', 'wound healing', 'cell-matrix adhesion, integrin-mediated signalling pathway', 'cell motion/migration', 'phospholipid binding', 'regulation of apoptosis' and 'adaptive immune response' (Fig. 7A), while 'glucose metabolic process', 'glycolysis' and 'growth factor activity' were enriched GO terms for down-regulated genes in 3-month-old DMD pigs (Fig. 7B). The full list of enriched GO terms of DEGs between 3-month-old DMD and WT pigs is shown in Supplementary Material, Table S2A and B. These molecular changes reflect the progressive muscular dystrophy in 3-month-old DMD pigs, involving degeneration, regeneration, inflammation and reactive fibrosis going along with a severe metabolic disturbance.

This was confirmed by functional annotation clustering of genes differentially expressed between 2-day-old and 3-month-old DMD pigs: enriched GO terms of genes with higher expression in 2-day-old DMD piglets, such as 'cofactor binding', 'mitochondrion', 'aerobic respiration', 'cellular respiration', 'carboxylic acid binding', 'FAD binding' and 'cofactor/coenzyme metabolic process' (Supplementary Material, Table S3A), are compatible with higher metabolic activity, while GO terms of genes with higher transcript levels in 3-month-old DMD pigs (Supplementary Material, Table S3B) reflect the processes of degeneration ('lysosome/vacuole', 'apoptosis'), regeneration ('tube morphogenesis', 'cell motion/migration', 'tube development'), inflammation ('immune response/inflammation', 'adaptive immune response', 'immunoglobulin receptor/binding', 'antigen processing and presentation', 'immunoglobulin') and fibrosis ('extracellular matrix', 'extracellular

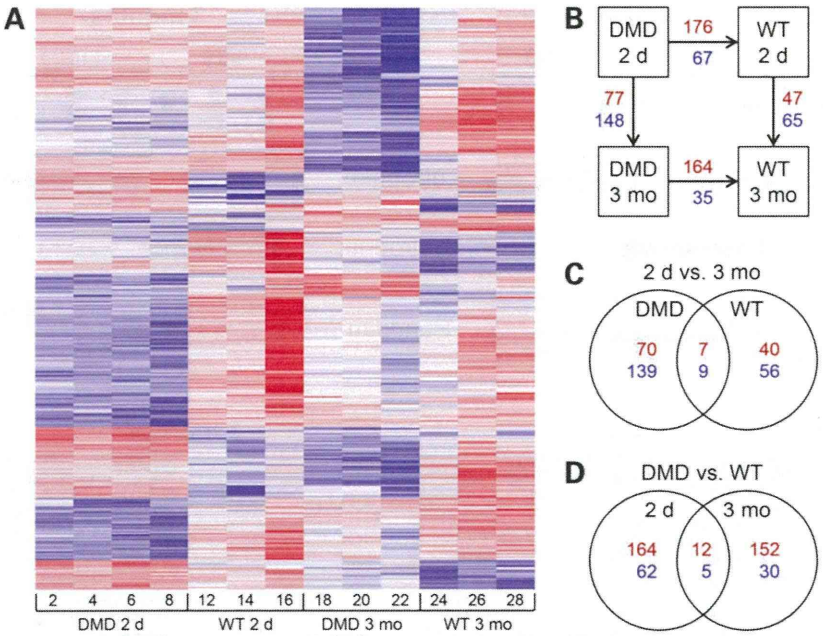

Figure 5. Differential gene expression in biceps femoris muscle of 2-day-old and 3-month-old DMD and WT pigs. (**A**) Heat-map of the DEGs among the four groups defined by genotype × age. Increased abundance of transcripts is indicated in red, decreased abundance in blue colours. (**B**) Number of DEGs between the four groups. Numbers in red and blue indicate the genes up- and down-regulated between the group at the end of an arrow versus the group at the arrow head. (**C**) Age-related transcriptome changes. The numbers in the overlap segment indicate DEGs commonly up- and down-regulated between 2-day-old and 3-month-old pigs of the DMD and WT groups. (**D**) Genotype-related transcriptome changes. The numbers in the overlap segment indicate DEGs commonly up- and down-regulated between DMD and WT pigs of both age classes.

structure organisation', 'collagen'). In WT pigs, the genes expressed at higher levels in 2-day-old animals were summarized by GO term 'extracellular matrix', while in 3-month-old animals transcripts belonging to GO terms 'muscle contraction', 'glucose metabolic process' and 'chloride ion binding' were more abundant (Supplementary Material, Table S4A and B).

Transcriptome changes in skeletal muscle of 3-month-old DMD pigs reflect human DMD and *mdx* mouse muscle

Next, we asked if the transcriptome changes observed in DMD pigs reflect the findings of gene expression studies in skeletal muscle of DMD patients and of the *mdx* mouse. Pescatori *et al.* (25) determined gene expression profiles in muscle biopsies of 19 DMD patients younger than 2 years, thus addressing the pre-symptomatic phase of the disease. Haslett *et al.* (26) investigated the transcriptome of skeletal muscle tissue in DMD children older than 5 years, when impaired muscle function and ambulation becomes clinically manifest. A systematic study of transcriptome changes in skeletal muscle of *mdx* mice between 7 and 112 days of age was performed by Porter *et al.* (27). To compare the changes in gene expression profiles of muscle samples from 2-day-old and 3-month-old DMD pigs versus age-matched controls with these published data sets, we performed gene set enrichment analyses (GSEAs) (28) providing a measure (normalized enrichment score, NES) of the concordance of DEG sets.

The transcripts with increased abundance in 3-month-old DMD pigs were in good concordance with the genes found to be up-regulated in DMD children younger than 2 years (25) (Fig. 7C), older than 5 years (26), and in *mdx* mouse muscles at 23 and 28 days of age (27) (Supplementary Material, Fig. S3A), as indicated by NES >2 with q-values of less than 0.001. A similarly good concordance was found for the down-regulated genes (Supplementary Material, Fig. S3B).

Transcriptomics of 2-day-old DMD pig muscle identifies a mechanical stress signature

The gene expression profiles of biceps femoris muscle samples from 2-day-old DMD piglets were rather different from the published sets of DEGs in DMD patients and in *mdx* mouse muscles (Supplementary Material, Fig. S3C). Specifically, samples from 2-day-old DMD pigs did not display the characteristic transcriptome signatures of ECM remodelling, inflammatory response and decreased energy metabolism which were observed even in DMD patients younger than 2 years, i.e. in the pre-symptomatic period. Instead, the set of transcripts with increased abundance in 2-day-old DMD piglets was similar to a set of genes up-regulated in muscle after acute exercise injury in humans (29) (Fig. 6C) and to transcripts induced by contractile overload (high-force eccentric contractions) in murine skeletal muscle (30) (NES = 1.7624; $q = 0.002$; data not shown).

DISCUSSION

In this study, we generated the first pig model for a genetic muscle disease by gene targeting. In mouse (31) and human

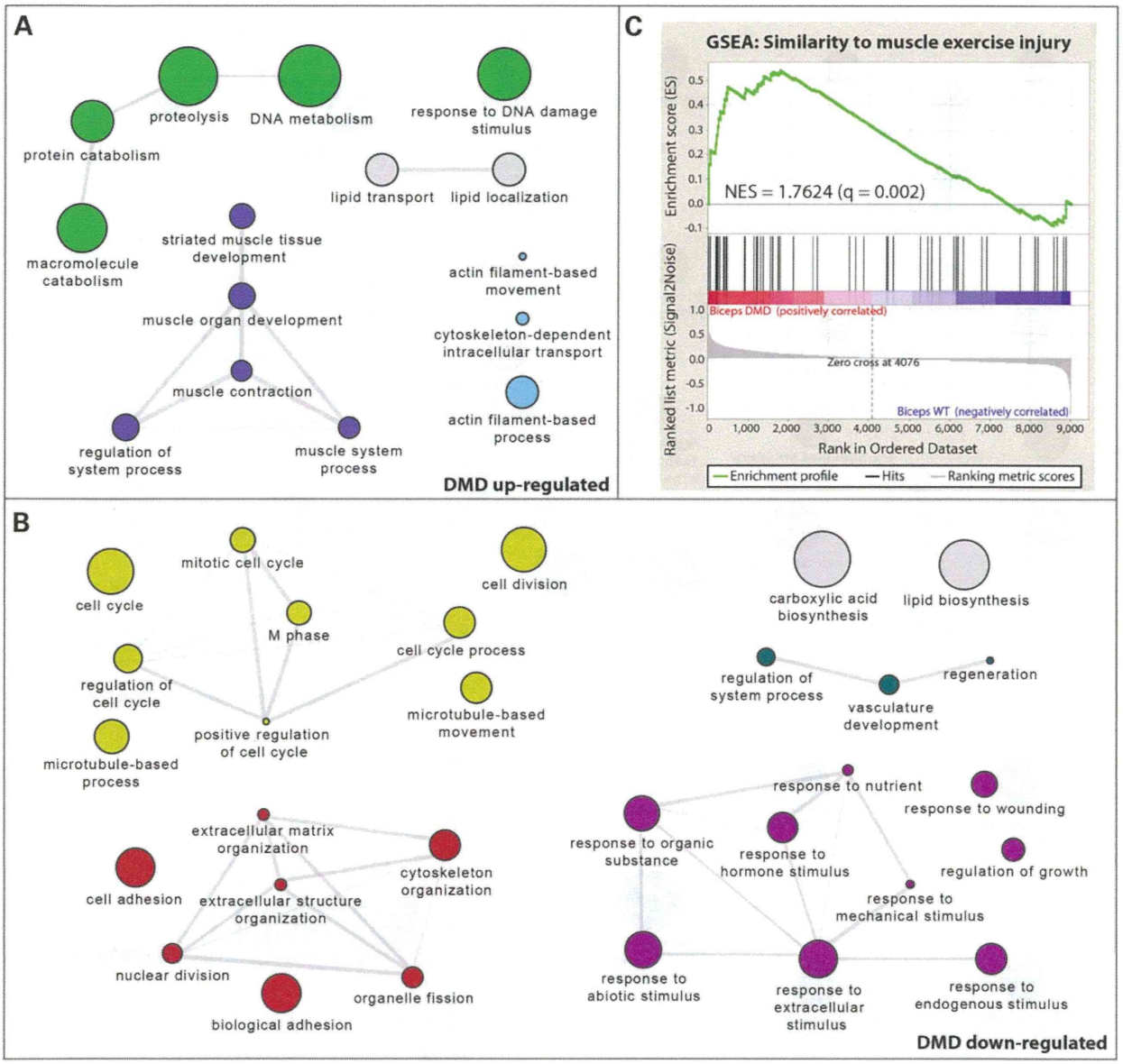

Figure 6. Graph-based visualization of enriched GO terms of genes differentially expressed between DMD and WT pigs at the age of 2 days. (**A**) GO terms of up-regulated and (**B**) GO terms of down-regulated genes in DMD versus WT pigs. The graphs were produced from all significantly enriched GO terms found by DAVID functional annotation clustering using the tools REVIGO (23) and Cytoscape (24). Each GO term is a node in the graph, and 3% of the strongest GO term pairwise similarities are designated as edges in the graph. The generality of GO terms is indicated by bubble size, with smaller bubbles implying more specific terms. (**C**) Gene set enrichment analysis of DEGs up-regulated in 2-day-old DMD pigs versus age-matched WT pigs in a set of genes up-regulated in human skeletal muscle exposed to acute endurance exercise (29). The enrichment profile (green curve) shows a non-random distribution indicated by a roughly triangular outline and a peak close to one of the extremes of the signal-to-noise ordered data set. This distribution means that a higher proportion than expected under the null hypothesis of the genes up-regulated in human skeletal muscle after acute endurance exercise is up-regulated in DMD pigs and fewer than expected are down-regulated or neutral. The leading edge subset containing the most up-regulated genes are the genes positioned left of the peak in the enrichment curve profile. The NES was calculated as outlined in the Materials and Methods section. The q-value is the false discovery rate (FDR) corrected P-value.

embryonic stem cells (32), a high rate of homologous recombination was observed with large targeting vectors based on BACs, avoiding the need for isogenetic DNA and negative selection markers (reviewed in 33). Therefore, we used a BAC containing the porcine *DMD* exon 52 and replaced it by recombineering (16). After nucleofection of the modified BAC into pre-tested nuclear donor cells, exon 52 replacement was observed in around 2% of the stable nucleofected cell clones, rendering BAC targeting an attractive method for introducing targeted mutations into large animal genomes. Importantly, the two targeted cell clones used for nuclear transfer produced pregnancies and offspring at a rate within the usual range of nuclear transfer in

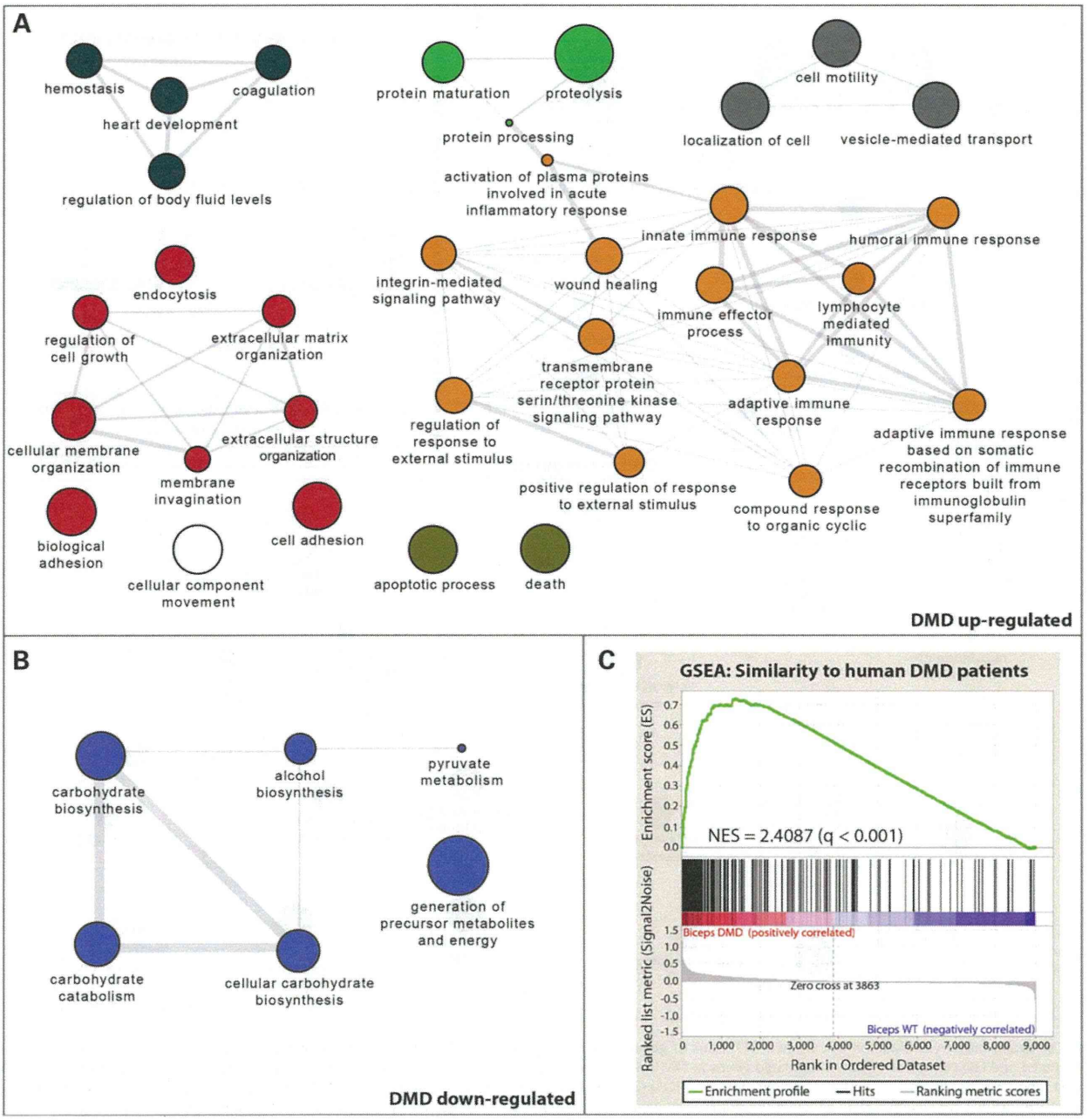

Figure 7. Graph-based visualization of enriched GO terms of genes differentially expressed between DMD and WT pigs at the age of 3 months, and comparison with a transcriptome study of DMD patients. (**A**) GO terms of up-regulated and (**B**) GO terms of down-regulated genes in DMD versus WT pigs. The graphs were produced from all significantly enriched GO terms found by DAVID functional annotation clustering using the tools REVIGO (23) and Cytoscape (24) as explained in legend of Figure 6. (**C**) Gene set enrichment analysis of DEGs up-regulated in 3-month-old DMD pigs versus age-matched WT pigs in a set of genes up-regulated in skeletal muscle of DMD boys younger than 2 years (25). The enrichment profile (green curve) shows a non-random distribution indicated by a roughly triangular outline and a peak close to one of the extremes of the signal-to-noise ordered data set. This distribution means that a higher proportion than expected under the null hypothesis of the genes up-regulated in DMD boys is up-regulated in DMD pigs and fewer than expected are down-regulated or neutral. The leading edge subset containing the most up-regulated genes are the genes positioned left of the peak in the enrichment curve profile. The NES was calculated as outlined in the Materials and Methods section. The q-value is the false discovery rate (FDR) corrected P-value.

the pig (34), demonstrating that BAC targeting and selection of single clones do not interfere with the potential of donor cells to yield cloned offspring.

Pigs lacking *DMD* exon 52 displayed a complete loss of dystrophin, as it is the case in the majority of DMD patients (17). In addition, the levels of dystrophin-associated glycoproteins

α-sarcoglycan and β-dystroglycan were reduced, mirroring the situation in DMD patients.

The DMD pig appears to be a bona fide model of the human dystrophy as ascertained by the absence of the dystrophin protein, elevated serum CK and progressive muscular dystrophy. The percentage of muscle fibre cross-sections with central nuclei (~10%) in 3-month-old DMD pigs appeared rather low when compared with *mdx* mice of the same age (~60%) (35). This might on the one hand reflect a lower regenerative potential of porcine DMD muscles, and might contribute to the accelerated severe muscle phenotype seen in DMD pigs when compared with *mdx* mice. On the other hand, the low percentage of muscle fibres with central nuclei might reflect the young age of the investigated pigs. Likewise, studies in *mdx* mice show that the percentage of muscle fibres with central nuclei increases with age (36). Another important point is that in *mdx* mouse muscle the myonuclei remain central for a long time after regeneration and can thus be used as a marker for regenerated muscle fibres, while in larger mammals the majority of nuclei in regenerating muscle fibres quickly become subsarcolemmal (reviewed in 37). Thus the higher percentage of central nuclei in the *mdx* mouse when compared with the DMD pig may reflect the difference in post-regenerative remodelling in the two species.

In addition to progressive muscle pathology, DMD pigs show characteristic disturbances of locomotion, including the inability in climbing a platform, which is comparable with the early difficulties of DMD patients in climbing stairs. It appears that DMD pigs exhibit the pathological and functional hallmarks of the human disease, but develop them in an accelerated mode. This offers improved opportunities for early and clear-cut readouts in efficacy studies of new treatments when compared with currently available animal models.

Our findings raise the questions (i) why disease progression in DMD pigs is markedly accelerated when compared with human patients; and (ii) why the severity of muscular dystrophy was associated with birth weight of DMD pigs.

Up-regulation of utrophin at the sarcolemma is a common observation in dystrophin-deficient human and mouse muscle (reviewed in 20). Functional compensation of dystrophin deficiency by utrophin has been demonstrated by amelioration of the pathology in *mdx* mice expressing utrophin transgenes (38,39) and by the fact that double mutant mice lacking both dystrophin and utrophin present a more severe phenotype than mice lacking only one of these proteins (40). Thus we asked whether the rapidly progressing muscular dystrophy of DMD pigs is due to a lack of sarcolemmal utrophin up-regulation. Since increased levels of utrophin have been observed in regenerating, dystrophin-deficient, or inflamed muscle without a corresponding increase in *UTRN* mRNA (41), we compared utrophin expression between DMD and WT pigs on the protein level by western blot and immunohistochemistry. While in muscle specimens of 3-month-old pigs, the sarcolemma stained clearly positive for utrophin, we did not detect sarcolemmal utrophin expression in 2-day-old DMD pigs. The utrophin expression pattern in DMD pigs reflects the situation in humans where young cases of DMD show very little sarcolemmal utrophin, but as the disease progresses utrophin is detectable on many mature muscle fibres (reviewed in 42).

Consistent with these findings, sarcolemmal utrophin was markedly increased in canine X-linked muscular dystrophy (CXMD) in skeletal muscle of 30- and 60-day-old and adult dystrophic animals (43). Moreover, in these dogs, utrophin expression was more persistent when compared with controls and female carriers. In the Golden Retriever muscular dystrophy (GRMD) animal model, a high mortality rate was observed during the first 2 weeks of life (44). Notably, utrophin immunostaining was absent, faintly or variably positive in skeletal muscle from 2-day-old dystrophic CXMD animals which died spontaneously. Similarly absent or variable utrophin expression was reported in puppies which died after days 8, 9 and 11 (43). In line with the findings in neonates of the canine muscular dystrophy model, the lack of sarcolemmal utrophin up-regulation in the 2-day-old DMD pig muscle may contribute to the lethality of some animals shortly after birth.

To gain insight into the hierarchy of disease mechanisms of muscular dystrophy of DMD pigs, we performed a holistic transcriptome analysis of skeletal muscle specimens from 2-day-old and 3-month-old animals. The muscle transcriptome changes of 3-month-old DMD pigs were very similar to those reported for muscle samples of DMD patients, demonstrating that the DMD pig reflects the human disease on the molecular level. In contrast, the transcriptome profile of skeletal muscle from 2-day-old DMD pigs was rather different from published transcriptome data sets of human DMD muscle. Interestingly, *CCL2*—coding for CC chemokine ligand 2, a ligand of CC chemokine receptor 2 (CCR2)—was one of the most down-regulated transcripts in 2-day-old DMD pigs. Experiments in *Ccl2* knockout mice demonstrated that CCL2 deficiency results in reduced inflammation and impaired regeneration after acute muscle injury (45). Further, $Ccl2^{-/-}$ mice exhibited reduced expression of *Igf1*, which was also seen in 2-day-old DMD pigs. In contrast, *CCL2* transcript levels were elevated in 3-month-old versus 2-day-old DMD pigs associated with marked inflammatory and regenerative processes. Thus *CCL2* is an interesting candidate to be involved in the transition from the early lesions observed in 2-day-old DMD piglets to the severe muscular dystrophy observed in 3-month-old DMD pigs with all clinical and pathological hallmarks of human DMD.

A classical hypothesis regarding the pathophysiology of dystrophin deficiency is that abnormal fragility and leakiness of the muscle cell membrane represents the initial pathology of DMD, which is made worse by mechanical stress (reviewed in 20). A primary role of mechanical stress in early DMD pathology is supported by the fact that the set of transcripts with increased abundance in 2-day-old DMD piglets was similar to a set of genes up-regulated in muscle after acute exercise injury (29,30). Our observation that the survival time of DMD pigs was inversely associated with birth weight (Fig. 2A) points to an effect of intrauterine and postnatal growth rate on the severity of the disease. Human foetal growth reaches a maximum between 30 and 36 weeks and declines thereafter as the mother fails to meet the increasing energy demand of her growing foetus. In contrast, pig foetuses have not reached their peak growth rate at birth and can double their birth weight within 7–10 days due to high rates of protein deposition and lean tissue growth and a marked increase in body fat, while human babies need 5 months to double their birth weight (reviewed in 46). Thus, the pig is a model of accelerated growth, which may aggravate the phenotypic consequences of DMD deficiency via different routes. Foetal pig muscles grow by hypertrophy from around day 75 of pregnancy (47). Since

mechanical strains per unit surface area increase with the calibre of muscle fibres (48), rapid muscle growth may render muscle fibres of DMD pigs particularly susceptible to sarcolemmal damage. Recently, Grounds and Shavlakadze (49) proposed that the sarcolemma of an actively growing myofibre has different properties to the sarcolemma of a mature adult myofibre and that the timing and pattern of muscle fibre growth affects the severity of phenotype of DMD deficiency. This concept is fully supported by the pathology of the DMD pig. Parturition is another potential source of mechanical stress on the muscle fibres which is expected to be proportionate to body weight. This hypothesis is supported by the observation that DMD pigs with a very high birth weight were most severely affected and could not move at all (Fig. 2A and Supplementary Material, Video S2). A third source of mechanical stress on the muscle fibres of DMD pigs may result from the fact that they start to move on their own shortly after birth, resulting in greater mechanical strains on the muscle fibres when compared with human DMD newborns. As the mechanical stress due to movement is expected to be correlated with body weight, this would also explain the longer survival of DMD pigs with low birth weight when compared with pigs with normal or high birth weight. In the genetic background used for our DMD model, the birth weight of wild-type piglets generated by breeding usually ranges between 1.0 and 1.8 kg, depending on litter size. Only three DMD piglets had birth weights slightly higher than 1.8 kg (Fig. 2A), arguing against the notion that the cloning process may have indirectly—by increasing birth weight—aggravated the phenotypic consequences of the *DMD* mutation. Using a genetic background with reduced growth rate might decelerate the DMD pathology and facilitate longer survival. Interestingly, the DMD piglets surviving up to 3 months showed a low postnatal growth rate and a markedly reduced body weight at 3 months when compared with age-matched controls (15.49 ± 1.63 versus 42.60 ± 3.66 kg; $P < 0.001$).

In summary, pigs lacking *DMD* exon 52 display progressive and—compared with DMD patients—markedly accelerated muscular dystrophy. Our transcriptome studies of skeletal muscle samples from young (2 days) and older (3 months) DMD pigs provide new insights into early changes associated with dystrophin deficiency and secondary changes during postnatal development, and thus into the hierarchy of physiological derangements in a severe dystrophin-deficient animal model. Since loss of exon 52 is a frequent mutation in human DMD and can be treated by exon 51 skipping (50), our pig model has potential for testing and refinement of this therapeutic strategy. In order to provide sufficient numbers of DMD pigs for systematic treatment trials, we successfully generated $DMD^{+/\Delta exon52}$ female cells and are currently using them for nuclear transfer to produce heterozygous females, which are expected to have 50% male DMD offspring. These may prove helpful in developing new therapies for muscular dystrophy, including exon skipping, gene and stem cell therapies.

MATERIALS AND METHODS

BAC targeting

Exon 52 of the porcine *DMD* gene was identified on BAC clone CH242-9G11. We replaced the exon by a neomycin resistance cassette (*neo*®) using bacterial recombineering (16). The homologous arms for recombineering were amplified by the primer pairs 5′-atg agc tct taa tta agg tgt tct ctc ctc tat g-3′ and 5′-tgg atc ctc gcg act gca gcc tta gaa gca gtc tcc ttc-3′ as well as 5′-atg gat ccg cgg ccg caa act gga acc aca aga c-3′ and 5′-atg gta cct taa tta atc tgc tct ctg gtc act c-3′. After endotoxin-free preparation of a correctly modified BAC and its linearization with *Sfi*I, 5–10 μg of the modified BAC was nucleofected into primary kidney cells (51) from a 3-month-old male piglet. Cells were selected with 1.2 mg/ml G418 in Dulbecco modified Eagle medium supplemented with 15% fetal bovine serum (FBS), 293 mg/l L-glutamine, antibiotics and 0.1 mM 2-mercaptoethanol and neomycin-resistant clones were expanded for screening and nuclear transfer.

Screening of clones was performed by qPCR using the target site specific primer pair 5′-tgc aca atg ctg gag aac ctc a-3′ and 5′-gtt ctg gct tct tga ttg ctg g-3′ as well as the reference primer pairs 5′-tgt ctg cga ccc aca cca-3′ and 5′-gca tgc atc agt aag gaa ctg g-3′ and 5′-tca tca gtg gat tca ccc caa-3′ and 5′-cac cac ggg aat gcc ttc-3′.

Nuclear transfer and embryo transfer

All animal procedures in this study were approved by the local Animal Welfare Committee (Regierung von Oberbayern) and were performed according to the German Animal Welfare Act and the European Communities Council Directive of 24 November 1986 (86/609/EEC). Two *DMD* mutant cell clones were used for somatic cell nuclear transfer according to Kurome *et al.* (52) with minor modifications. HEPES-buffered medium 199 plus 10% FBS was used for all manipulations and post-activation culture. Fusion was done in Eppendorf fusion medium using the Multiporator® device (Eppendorf, Hamburg, Germany). Embryo transfer was performed as previously described (53). The second round of nuclear transfer experiments was done with the *DMD* targeted cell clone used to generate piglet #1263 or primary kidney cells from #1263 as nuclear donors.

Genotyping and clinical chemistry

Genotyping of the animals was done by PCR analysis of DNA isolated from fibroblast cell cultures established from ear biopsies. Target site specific primers 5′-cag cag cag tca aag ggc ata-3′ and 5′-agg caa gtc tgg gaa gca tca-3′ were applied for detection of exon 52 of the *DMD* gene. The primer pair 5′-cgc tcg tgg tcg aca acg-3′ and 5′-ctg gat ggc cac gta cat g-3′ designed on the sequence of the *ACTB* gene was used as a reference. PCR products were separated on a 2% agarose gel and stained with ethidium bromide. Serum CK levels were determined using the Hitachi 912E Automatic Analyser (Roche Diagnostics, Mannheim, Germany).

RNA sequencing and bioinformatics

Total RNA from two newborn *DMD* knockout piglets and two wild-type controls was isolated from cryopreserved tissue samples using Trizol® (Invitrogen, Carlsbad, CA, USA). Purity and integrity of RNA was assessed by spectrophotometry (nanodrop ND-100, Nanodrop, Wilmington, USA) and agarose gel electrophoresis. Fifty nanograms of total RNA was used for random primed cDNA synthesis and isothermal amplification

using the Ovation RNA-Seq kit (Nugen, San Carlos, CA, USA). The primers p50f7361 (5′-aga aag tta gaa gat ctg agc-3′) and p53r7879 (5′-ttg cct tct gtt ctg aag g-3′) were used for cDNA amplification. Amplified double-stranded cDNA was end-repaired and ligated to bar-coded adapters provided with the Encore Multiplex Kit (Nugen). Finally, the adapter ligated library was enriched and amplified by 10 PCR cycles according to the kit protocol. Concentration and size distribution of the library was determined with a DNA1000 chip on a 2100 Bioanalyser (Agilent, Santa Clara, CA, USA). The four bar-coded libraries were mixed at equimolar amounts and sequenced on one lane of Illumina's Genome Analyser IIx in single read mode and 75 nucleotides read length. Sequence reads were de-multiplexed according to a four-base leading bar-code and mapped to the pig genome (susScr2 from UCSC genome browser) with the spliced-read aligner Tophat v1.2.0 (54). Normalized read counts (FPKM, fragments per kilobase of transcript and per million mapped reads) based on the Ensembl annotation were calculated with Cuffdiff (v1.0.3) from the Cufflinks program package (55).

Microarray analysis

Total RNA from seven *DMD* knockout piglets and six wild-type controls was isolated from RNAlater preserved M. biceps femoris samples using Trizol® (Invitrogen). Purity and integrity of RNA was assessed by spectrophotometry (nanodrop ND-100, Nanodrop) and Agilent Bioanalyser 2100 (Agilent). Two hundred nanograms of total RNA was used for cDNA synthesis, amplification, fragmentation and labelling using the Nugen Applause WTA ST and Encore Biotin labelling kits (Nugen, San Antonio, TX, USA). Labelled probes were hybridized to Affymetrix PorGene 1.0 ST GeneChips, washed, stained in an Affymetrix FS450 station and scanned on an Affymetrix GeneChip Scanner 3000 (Affymetrix, Santa Clara, CA, USA). The array CEL-files were RMA normalized by apt tool from Affymetrix and analysed for differential expression in R using the limma package. Gene annotations were extended by their orthologous human gene symbol. Porcine transcripts (susScr10.2) were aligned against the human transcripts (hg19) using BLAST and best matching hits with a bit score > 80 were accepted. Genes were regarded as differentially expressed when passing the thresholds of fdr < 0.05 and $\log_2$fold-change > 1. Functional analysis of DEGs was done by DAVID functional annotation clustering (21,22) with an enrichment score of ≥ 1.3, REVIGO (23) and Cytoscape (24) for summarization and visualization of GO annotations obtained by functional annotation clustering from DAVID, and GSEA (28). As a measure of concordance between sets of DEGs, the NES was used, which accounts for differences in gene set size and in correlations between gene sets. The normalization allows for comparison across gene sets.

Immunoblot analysis

Muscle tissue was homogenized in lysis buffer [125 mM Tris pH 8.8, 40% glycerol, 4% SDS, 0.5 mM PMSF, 100 mM DTT, Complete® protease inhibitor (Roche), bromophenol blue] (56), and protein concentration was determined by the Pierce 660 nm Protein Assay (Thermo Fisher Scientific, Rockford, IL, USA). Defined amounts of total muscle protein were separated by 5% SDS–PAGE and blotted to PVDF membrane. Dystrophin and dysferlin were detected using mouse monoclonal antibodies (NCL-DYS1 and NCL-DYS2, dilution 1:400, Novocastra, Newcastle upon Tyne, UK; and NCL-Hamlet, dilution 1:1000, Novocastra, respectively) and horseradish peroxidase-coupled polyclonal goat anti-mouse antibodies (115-035-146, dilution 1:10 000, Jackson ImmunoResearch, Suffolk, UK). Utrophin was detected using polyclonal rabbit anti-utrophin (sc-15377, dilution 1:800, Santa Cruz Biotechnology, Heidelberg, Germany) and horseradish peroxidase-coupled polyclonal goat anti-rabbit antibodies (dilution 1:2000, Cell Signaling). Bound antibodies were visualized using ECL reagent (RPN2106; GE Healthcare Amersham Biosciences, Freiburg, Germany).

Locomotion studies

A kinematic gait analysis was performed in a 9-week-old *DMD* mutant pig and a size-matched wild-type control using a digital video camera. The animals were trained to move in a linear test track (15 m long, 80 cm broad), which was built by spanning a wire fence in front of a wall. The animals were provoked to walk, trot or gallop by offering food as an incentive. The videos were evaluated in real time and time lapse, taking various kinematic parameters, such as stride length, stride speed, swing and stance phase, regularity and rhythm into account. In addition, the ability to jump up and down a small platform (height: 25 cm) was evaluated. The video is provided in full length as Supplementary Material, Video S1. A second set of kinematic movement analyses was performed on three 10-week-old DMD pigs and a size-matched control.

Necropsy and histopathology

DMD-deficient pigs which had to be euthanized due to progressive worsening were necropsied, and tissue samples of the left and right biceps femoris muscle, triceps brachii muscle, longissimus dorsi muscle, thyreohyoideus muscle, of the diaphragm (left pillar), intercostal muscles and the left heart ventricle were taken for histological examination. Control tissues were obtained from age-matched male wild-type pigs. In total, 22 DMD-deficient pigs [aged 1 day ($n = 6$), 2 days ($n = 4$), 3 days ($n = 3$), 4 days ($n = 1$), 1 week ($n = 1$), 2 weeks ($n = 1$), 7 weeks ($n = 1$) and 3 months ($n = 5$)], and six healthy male wild-type pigs [2 days ($n = 3$) and 12 weeks of age ($n = 3$)] were investigated. Samples were routinely fixed in neutrally buffered formaldehyde solution (4%) for 24 h. Formalin-fixed tissue specimens were embedded in paraffin or in plastic (glycol methacrylate and methyl methacrylate; GMA/MMA) (57). Cross and longitudinal muscle sections were stained with haematoxylin and eosin (H&E), or Masson's trichrome-stain, respectively.

Immunofluorescence and immunohistochemical studies

For immunofluorescence studies, samples of the biceps femoris muscle, triceps brachii muscle, longissimus dorsi muscle, diaphragm and heart from DMD pigs and age-matched wild-type control animals were immersed in 10% gum tragacanth (Sigma-Aldrich, Taufkirchen, Germany) and immediately frozen in liquid nitrogen-cooled isopentane (−150°C). Immunofluorescence studies were performed on 8 μm thick frozen sections. Primary antibodies used in this study were